

# Failure Model for Unidirectional Fiber Reinforced Composites

EMILIA SABAU<sup>1</sup>, HORATIU IANCAU<sup>1</sup>, LIANA HANCU<sup>1</sup>, MARIAN BORZAN<sup>1</sup>, STEFAN GRIGORAS<sup>2</sup>

<sup>1</sup>Technical University of Cluj-Napoca, 15 Daicoviciu, 400020, Cluj-Napoca, Romania.

<sup>2</sup>Gh. Asachi Technical University of Iasi, 61 Mangeron, 700050, Iasi, Romania

*This paper presents a failure model applicable for unidirectional fibers reinforced composites that point out the fiber-matrix interface role in the mechanics of the failure process. The model is applicable in any plane stress state case. The ABAQUS/Standard finite elements program is used to point out the applicability of failure model. The deformation of a square plate with the dimensions of 100x100 mm, having a hole with the diameter of 50 mm in the middle, was analyzed. The plate is realized from composite materials with unidirectional fibers oriented at an angle of 45°. The visualization and the interpretation of the simulation results have been made with the help of ABAQUS/Viewer module. The obtained diagrams reflect a very good concordance between the predictions of the failure model and the results provided by other models. This confirms the hypothesis on whose basis the unidirectional composite failure model was formulated.*

*Keywords: composite materials, failure, unidirectional fiber glass, polyester resin*

The attempts to obtain new materials with high performance lead to the development of a product class known under the name of composite materials. According to the components' nature and structure, as well as according to the adhesion between the layers, the polymeric composite materials have very different properties. Thus, we can attain very rigid or very flexible materials, with high resistance at traction, bending or shock trials, with resistance at very low or very high temperatures, electro-conductor or insulating, or even unflamable materials [1].

The failure of composite materials can occur in a wide range of ways [6], including:

- fibers failure - generally occurs under the action of traction loads;
- matrix micro-failure - indicates the appearance of microscopic cracks into the polymeric matrix (they can be caused by the mechanical loading, by the remanent stresses that were induced after the thermal treatment process, by the absorption of humidity or by the seasoning of the matrix material);
- matrix failure - is similar to the micro-failure, but the cracks are larger, since they have the dimensions of the fiber's diameter (or higher);
- the destruction of the fiber-matrix bond - when the reinforce fibers are separated by the matrix;
- the exfoliation or the layers of a laminate (delamination).

These types of failure develop according to the material nature and to the conditions of the mechanical sollicitation.

## Failure model for unidirectional composites

This paper presents an original failure model applicable for unidirectional glass fibers reinforced composites (unidirectional glass fibers 225 g/m<sup>2</sup>/polyester) [2, 4, 5]. The model starts from the premise that the failure happens due to the destruction of the fiber-matrix bond. Figure 1 presents a plate of composite material with unidirectional glass fibers orientated at a certain  $\theta$  angle. The failure model is based on the following hypothesis:

- the plate in its whole remains in plane stress state throughout the deformation;

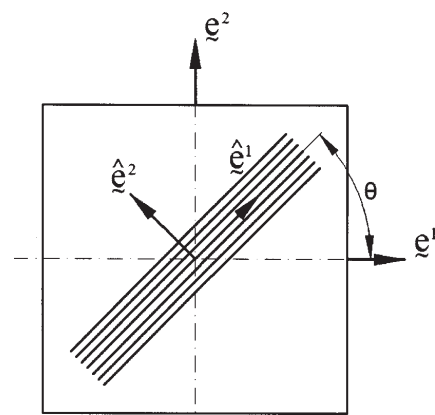


Fig. 1. Composite materials plate with unidirectional fibers

- the model of plane stress state approximates the phenomena that occurs in the matrix, respectively in the fibers taken individually;
- the plate in its whole has a linear-elastic behaviour of orthotropic type;
- the matrix and the fibers taken separately have a linear-elastic behaviour of isotropic type.

We consider:

$(e^1, e^2, e^3)$  - orthonormal basis associated plate assembly;

$(\hat{e}^1, \hat{e}^2, \hat{e}^3)$  - orthonormal basis that defines the axes system of the elastic orthotropic plate;

$\theta \in [0^\circ, 180^\circ)$  - angle that defines the fiber orientation.

Cartesian decomposition of tension and strain tensors was exclusively used. This can be explained using the global basis  $(e^1, e^2, e^3)$ , and the orthotropic basis  $(\hat{e}^1, \hat{e}^2, \hat{e}^3)$ . The following presents the constitutive equations:

a. For the plate

$$\{\hat{\sigma}\} = [\hat{Q}]\{\hat{\epsilon}\} \quad (1)$$

The matrix's elements  $[\hat{Q}]$  have the following formulae:

\* Tel.: +40264401710

$$\begin{cases} \hat{Q}_{11} = \frac{E_1}{1 - \nu_{12}\nu_{21}} \\ \hat{Q}_{12} = \hat{Q}_{21} = \frac{\nu_{12}E_2}{1 - \nu_{12}\nu_{21}} = \frac{\nu_{21}E_1}{1 - \nu_{12}\nu_{21}}; \hat{Q}_{13} = \hat{Q}_{31} = 0 \\ \hat{Q}_{22} = \frac{E_2}{1 - \nu_{12}\nu_{21}}; \hat{Q}_{23} = \hat{Q}_{32} = 0 \\ \hat{Q}_{33} = G_{12} \end{cases} \quad (2)$$

b. For the fibers

$$\{\hat{\sigma}^{(f)}\} = [\hat{Q}^{(f)}]\{\hat{\varepsilon}^{(f)}\} \quad (3)$$

where  $[\hat{Q}^{(f)}]_{3 \times 3}$  is a symmetrical matrix, whose elements have the following formulae:

$$\begin{cases} \hat{Q}_{11}^{(f)} = \frac{E^{(f)}}{1 - [\nu^{(f)}]^2} \\ \hat{Q}_{12}^{(f)} = \hat{Q}_{21}^{(f)} = \frac{\nu^{(f)}E^{(f)}}{1 - [\nu^{(f)}]^2}; \hat{Q}_{13}^{(f)} = \hat{Q}_{31}^{(f)} = 0 \\ \hat{Q}_{22}^{(f)} = \frac{E^{(f)}}{1 - [\nu^{(f)}]^2}; \hat{Q}_{23}^{(f)} = \hat{Q}_{32}^{(f)} = 0 \\ \hat{Q}_{33}^{(f)} = \frac{E^{(f)}}{2[1 + \nu^{(f)}]} \end{cases} \quad (4)$$

c. For the matrix

$$\{\hat{\sigma}^{(m)}\} = [\hat{Q}^{(m)}]\{\hat{\varepsilon}^{(m)}\} \quad (5)$$

where  $[\hat{Q}^{(m)}]_{3 \times 3}$  is a symmetrical matrix, whose elements have the following formulae:

$$\begin{cases} \hat{Q}_{11}^{(m)} = \frac{E^{(m)}}{1 - [\nu^{(m)}]^2} \\ \hat{Q}_{12}^{(m)} = \hat{Q}_{21}^{(m)} = \frac{\nu^{(m)}E^{(m)}}{1 - [\nu^{(m)}]^2}; \hat{Q}_{13}^{(m)} = \hat{Q}_{31}^{(m)} = 0 \\ \hat{Q}_{22}^{(m)} = \frac{E^{(m)}}{1 - [\nu^{(m)}]^2}; \hat{Q}_{23}^{(m)} = \hat{Q}_{32}^{(m)} = 0 \\ \hat{Q}_{33}^{(m)} = \frac{E^{(m)}}{2[1 + \nu^{(m)}]} \end{cases} \quad (6)$$

Hypothesis

Fiber-matrix interface has a limited capacity to download the stress difference between both constituents of the composite.

The condition of the composite cohesion is defined as:

$$\{\hat{\sigma}^{(f-m)}\}^T [\hat{M}^{(f-m)}] \{\hat{\sigma}^{(f-m)}\} < 1 \quad (7)$$

where  $[\hat{M}^{(f-m)}]_{3 \times 3}$  is a symmetrical matrix, whose elements have the following formulae:

$$\begin{cases} \hat{M}_{11}^{(f-m)} = F \\ \hat{M}_{12}^{(f-m)} = \hat{M}_{21}^{(f-m)} = G; \hat{M}_{13}^{(f-m)} = \hat{M}_{31}^{(f-m)} = 0 \\ \hat{M}_{22}^{(f-m)} = H; \hat{M}_{23}^{(f-m)} = \hat{M}_{32}^{(f-m)} = 0 \\ \hat{M}_{33}^{(f-m)} = 2L \end{cases} \quad (8)$$

where F, G, H, L are constant material parameters specific to the fiber-matrix interface.

The loss of composite cohesion occurs when:

$$\{\hat{\sigma}^{(f-m)}\}^T [\hat{M}^{(f-m)}] \{\hat{\sigma}^{(f-m)}\} = 1 \quad (9)$$

The experimental data shows that the failure surfaces of the plates with unidirectional orientation have approximately a relatively ellipsoidal shape, the ellipsoidal axes being oriented parallel to the orthotropic axes. The matrix  $[\hat{N}^{(f-m)}]$  can model such a behaviour only if:

$$\hat{N}_{12}^{(f-m)} = \hat{N}_{21}^{(f-m)} = 0 \quad (10)$$

In order to identify the failure model, the following particular cases are considered:

$$\alpha = 0^\circ \Rightarrow \{V_0^{(u)}\} = [1, 0, 0]^T \Rightarrow \hat{N}_{11}^{(f-m)} = \left[ \frac{1}{\hat{\sigma}_{0^\circ}^{(u,cr)}} \right]^2 \Rightarrow$$

$$[\hat{T}_{11}^{(f-m)}]^2 F + 2\hat{T}_{11}^{(f-m)}\hat{T}_{21}^{(f-m)}G + [\hat{T}_{21}^{(f-m)}]^2 H = \left[ \frac{1}{\hat{\sigma}_{0^\circ}^{(u,cr)}} \right]^2 \quad (11)$$

$$\alpha = 90^\circ \Rightarrow \{V_{90^\circ}^{(u)}\} = [0, 1, 0]^T \Rightarrow \hat{N}_{22}^{(f-m)} = \left[ \frac{1}{\hat{\sigma}_{90^\circ}^{(u,cr)}} \right]^2 \Rightarrow$$

$$[\hat{T}_{12}^{(f-m)}]^2 F + 2\hat{T}_{12}^{(f-m)}\hat{T}_{22}^{(f-m)}G + [\hat{T}_{22}^{(f-m)}]^2 H = \left[ \frac{1}{\hat{\sigma}_{90^\circ}^{(u,cr)}} \right]^2 \quad (12)$$

$$\alpha = 45^\circ \Rightarrow \{V_{45^\circ}^{(u,cr)}\} = \frac{1}{2}[1, 1, 1]^T \Rightarrow$$

$$\hat{N}_{11}^{(f-m)} + \hat{N}_{12}^{(f-m)} + \hat{N}_{21}^{(f-m)} + \hat{N}_{22}^{(f-m)} + \hat{N}_{33}^{(f-m)} = \left[ \frac{2}{\hat{\sigma}_{45^\circ}^{(u,cr)}} \right]^2 \Rightarrow$$

$$\hat{N}_{33}^{(f-m)} = \left[ \frac{2}{\hat{\sigma}_{45^\circ}^{(u,cr)}} \right]^2 - \left[ \frac{1}{\hat{\sigma}_{0^\circ}^{(u,cr)}} \right]^2 - \left[ \frac{1}{\hat{\sigma}_{90^\circ}^{(u,cr)}} \right]^2 \Rightarrow \quad (13)$$

$$2[\hat{T}_{33}^{(f-m)}]^2 L = \left[ \frac{2}{\hat{\sigma}_{45^\circ}^{(u,cr)}} \right]^2 - \left[ \frac{1}{\hat{\sigma}_{0^\circ}^{(u,cr)}} \right]^2 - \left[ \frac{1}{\hat{\sigma}_{90^\circ}^{(u,cr)}} \right]^2$$

The condition (10) causes a fourth constraint applied to the material parameters F, G, H:

$$\hat{T}_{11}^{(f-m)}\hat{T}_{12}^{(f-m)}F + [\hat{T}_{11}^{(f-m)}\hat{T}_{22}^{(f-m)} + \hat{T}_{12}^{(f-m)}\hat{T}_{21}^{(f-m)}]G + \hat{T}_{21}^{(f-m)}\hat{T}_{22}^{(f-m)}H = 0 \quad (14)$$

The system solution of equations (11), (12), (13) and (14) is:

$$F = \frac{1}{[\hat{T}_{11}^{(f-m)}\hat{T}_{22}^{(f-m)} - \hat{T}_{12}^{(f-m)}\hat{T}_{21}^{(f-m)}]^2} \left\{ \left[ \frac{\hat{T}_{22}^{(f-m)}}{\hat{\sigma}_{0^\circ}^{(u,cr)}} \right]^2 + \left[ \frac{\hat{T}_{21}^{(f-m)}}{\hat{\sigma}_{90^\circ}^{(u,cr)}} \right]^2 \right\}$$

$$G = -\frac{1}{[\hat{T}_{11}^{(f-m)}\hat{T}_{22}^{(f-m)} - \hat{T}_{12}^{(f-m)}\hat{T}_{21}^{(f-m)}]^2} \left\{ \frac{\hat{T}_{12}^{(f-m)}\hat{T}_{22}^{(f-m)}}{[\hat{\sigma}_{0^\circ}^{(u,cr)}]^2} + \frac{\hat{T}_{11}^{(f-m)}\hat{T}_{21}^{(f-m)}}{[\hat{\sigma}_{90^\circ}^{(u,cr)}]^2} \right\}$$

$$H = \frac{1}{[\hat{T}_{11}^{(f-m)}\hat{T}_{22}^{(f-m)} - \hat{T}_{12}^{(f-m)}\hat{T}_{21}^{(f-m)}]^2} \left\{ \left[ \frac{\hat{T}_{12}^{(f-m)}}{\sigma_{0^\circ}^{(u,cr)}} \right]^2 + \left[ \frac{\hat{T}_{11}^{(f-m)}}{\sigma_{90^\circ}^{(u,cr)}} \right]^2 \right\}$$

$$L = \frac{1}{2[\hat{T}_{33}^{(f-m)}]^2} \left\{ \left[ \frac{2}{\sigma_{45^\circ}^{(u,cr)}} \right]^2 - \left[ \frac{1}{\sigma_{0^\circ}^{(u,cr)}} \right]^2 - \left[ \frac{1}{\sigma_{90^\circ}^{(u,cr)}} \right]^2 \right\} \quad (15)$$

The solution above exists if the following condition is considered:

$$\det[\hat{T}^{(f-m)}] = [\hat{T}_{11}^{(f-m)}\hat{T}_{22}^{(f-m)} - \hat{T}_{12}^{(f-m)}\hat{T}_{21}^{(f-m)}]\hat{T}_{33}^{(f-m)} \neq 0 \quad (16)$$

The failure model is identifiable only if the elastic properties of the fibers and the matrix are different.

### Failure model implementation in ABAQUS/Standard program

In order to highlight the applicability of the failure model presented above, for any geometric shape of parts made from composite materials (unidirectional glass fibers 225 g/m<sup>2</sup>/polyester), the ABAQUS/Standard [3, 7], simulation program based on finite elements analysis was used.

### Model hypothesis

The model is based on the following hypothesis:

- behaviour described by a linear orthotropic constitutive equation;
- failure described by the loss of fiber-matrix cohesion criterion;
- possibility for the material to take large deformations and rotations.

In order to evaluate the constitutive model performances, the deformation of a square plate with the dimensions of 100x100 mm, with a hole with the diameter of 50 mm in the middle was analyzed. The plate is realized

from composite materials with unidirectional glass fibers oriented at an angle of 45° towards the sides, a configuration that appears very frequent at the assembly of composite materials.

### Description of the material model (defined by routine UMAT intermediary)

Defining the constitutive model attached to the plate implied specifying the state variables number of the model (in this case, using a single variable, parameter of loss cohesion), specifying the materials constants of the model (Young modulus  $E$ , shear modulus  $G$  and Poisson coefficient  $\nu$  for fibers, matrix and composite), and also defining the sectional properties of the finite elements of the mesh of the plate.

Defining the sectional properties of the plate implied specifying the material thickness and name, respectively the coordinate system orientation that were associated with the orthotropic axes of the composite (in this case the fibers are orientated at 45°).

### Visualization and interpretation of simulation results

The visualization and the interpretation of the simulation's results have been made with the help of ABAQUS/Viewer module. This realizes the graphical representation of the numerical results provided by the ABAQUS/Standard solver.

Figure 2 presents the distribution of loss cohesion parameter at the start of the crack. On the diagram from figure 2, the maximum value equal to 1 defines the place of cracking point.

Figure 3 presents the distribution of von Mises equivalent stress in configuration of failure plate. It is observed that the maximum value of 88.48 N/mm<sup>2</sup> is located almost in the same position as the maximum of loss cohesion parameter (fig. 2).

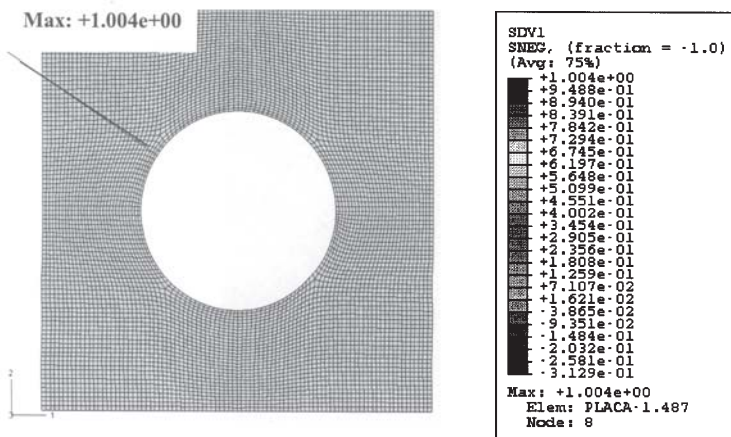


Fig. 2. Distribution of loss cohesion parameter at the cracking point

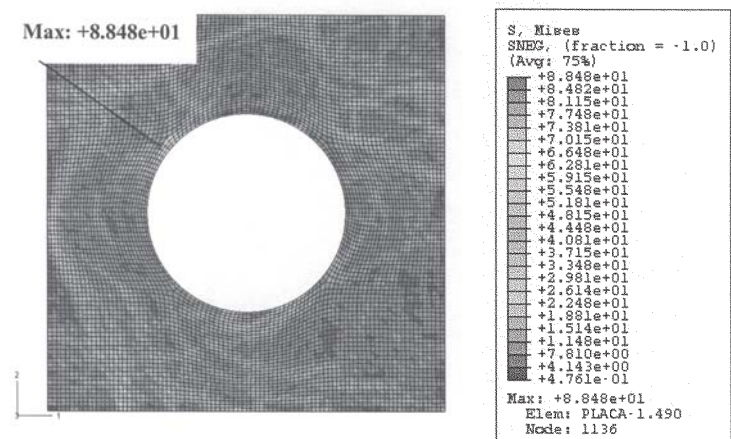


Fig. 3. Distribution of von Mises equivalent stress in configuration of failure plate

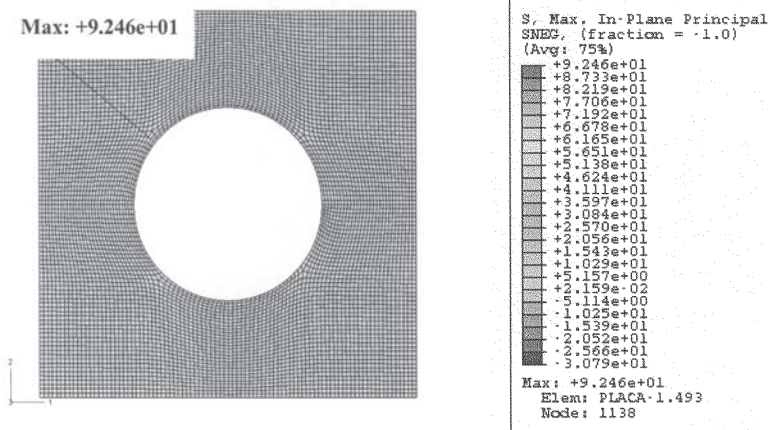


Fig. 4. Distribution of maximum main stress in configuration of plate failure

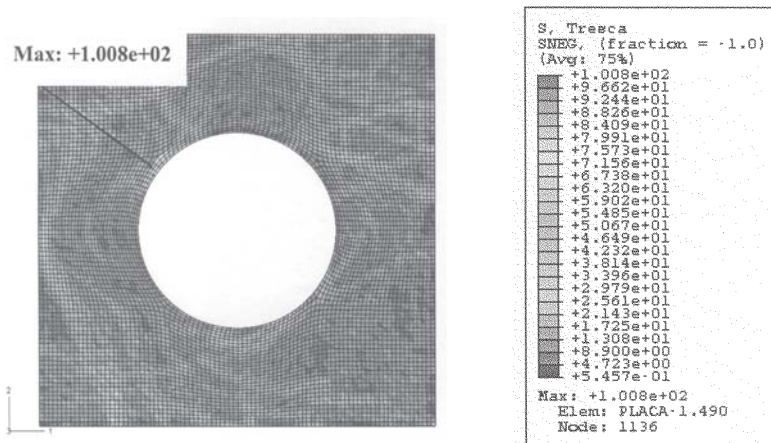


Fig. 5. Distribution of equivalent stress Tresca in configuration of plate failure

In the case of distribution of maximum main stress in configuration of plate failure (fig. 4), the maximum value is 92.46 N/mm<sup>2</sup> and, at the same time, it is located almost in the same position as the maximum of loss cohesion parameter.

For equivalent stress distribution Tresca (double of maximum tangential stress) in configuration of plate failure (fig. 5), maximum value is 100.8 N/mm<sup>2</sup>. Again, the maximum is located almost in the same position as the maximum of loss cohesion parameter.

### Conclusions

Through the realization of the failure model for a unidirectional fibers reinforced composite, we pointed out the role of the interface between fiber and matrix in the failure process. The model is applicable in any plane stress state case (uniaxial solicitations, respectively biaxial solicitations which may include shear components in the median area of the composite).

The presented example demonstrates the possibility to implement the proposed failure model in the structure of finite elements analysis programs.

The presented diagrams in figures 2 - 5 reflect a very good concordance between the predictions of the failure model and the results provided by other models (von Mises equivalent stress of maximum value criterion, maximum

main stress criterion, respectively maximum tangential stress criterion). This confirms the hypothesis on whose basis the unidirectional composite failure model was formulated.

The model can be used for dimensioning plates of composite structures and for establishing their mechanical resistance.

### References

1. IANCAU, H., NEMEȘ, O., Materiale compozite. Concepție și fabricație, Ed. Mediamira, Cluj-Napoca, 2003, p. 17
2. SABĂU, E., Contributions regarding mechanical behavior of composite structures with polymeric matrix, PhD. Thesis, Technical University of Cluj-Napoca, Romania, 2009, p. 115
3. ABAQUS 6.6. HTML Documentation 2008, (Electronically documentation).
4. KOLLÁR, L.P., SPRINGER, G.S., Mechanics of composite structures, Cambridge University Press, USA, 2003, p. 3
5. JONES, M.R., Mechanics of composite materials, Second Edition, Taylor & Francis, USA, 1999, p. 55-63, 106.
6. OPREA, V.C., CONSTANTINESCU, A., BĂRSĂNESCU, P., Ruperea polimerilor. Teorie și aplicații., Ed. Tehnică, București, 1992, p. 37
7. IANUS G., et all, The Effects of the Damaged Structure of Grease's Soaps on Ball Bearings Vibration. Rev. Plastic Materials Elastomers Syntetic Fibres, MPLAAM 44(1)1-96(2007), ISSN 0025-5289, p. 47

Manuscript received: 3.05.2010